

RESEARCH PAPER

Effects of atorvastatin metabolites on induction of drug-metabolizing enzymes and membrane transporters through human pregnane X receptor

E Hoffart¹, L Ghebreghiorgis², AK Nussler^{3,4}, WE Thasler⁵, TS Weiss⁶, M Schwab^{1,7} and O Burk¹

¹Dr Margarete Fischer-Bosch-Institute of Clinical Pharmacology, Stuttgart and University of Tübingen, Tübingen, Germany, ²Institute of Technical Biochemistry, University of Stuttgart, Stuttgart, Germany, ³Universitätsmedizin Berlin, Department of Surgery, Charité, Campus-Virchow-Clinic, Berlin, Germany, ⁴Department of Traumatology, University of Tübingen, Tübingen, Germany, ⁵Centre of Liver Cell Research, Department of Surgery, Ludwig-Maximilians-University Munich, Hospital Grosshadern, Munich, Germany, ⁶Department of Paediatrics and Juvenile Medicine, University of Regensburg Hospital, Regensburg, Germany, and ⁷Department of Clinical Pharmacology, Institute of Experimental and Clinical Pharmacology and Toxicology, University Hospital, Tübingen, Germany

Correspondence

Dr Oliver Burk, Dr Margarete Fischer-Bosch-Institute of Clinical Pharmacology, Auerbachstrasse 112, D-70376 Stuttgart, Germany.
E-mail:
oliver.burk@ikp-stuttgart.de

Keywords

atorvastatin; metabolites; *para*-hydroxy atorvastatin; PXR; CAR; induction; drug interaction

Received

18 March 2011

Revised

16 August 2011

Accepted

26 August 2011

BACKGROUND AND PURPOSE

Atorvastatin metabolites differ in their potential for drug interaction because of differential inhibition of drug-metabolizing enzymes and transporters. We here investigate whether they exert differential effects on the induction of these genes via activation of pregnane X receptor (PXR) and constitutive androstane receptor (CAR).

EXPERIMENTAL APPROACH

Ligand binding to PXR or CAR was analysed by mammalian two-hybrid assembly and promoter/reporter gene assays. Additionally, surface plasmon resonance was used to analyse ligand binding to CAR. Primary human hepatocytes were treated with atorvastatin metabolites, and mRNA and protein expression of PXR-regulated genes was measured. Two-hybrid co-activator interaction and co-repressor release assays were utilized to elucidate the molecular mechanism of PXR activation.

KEY RESULTS

All atorvastatin metabolites induced the assembly of PXR and activated CYP3A4 promoter activity. Ligand binding to CAR could not be proven. In primary human hepatocytes, the *para*-hydroxy metabolite markedly reduced or abolished induction of cytochrome P450 and transporter genes. While significant differences in co-activator recruitment were not observed, *para*-hydroxy atorvastatin demonstrated only 50% release of co-repressors.

CONCLUSIONS AND IMPLICATIONS

Atorvastatin metabolites are ligands of PXR but not of CAR. Atorvastatin metabolites demonstrate differential induction of PXR target genes, which results from impaired release of co-repressors. Consequently, the properties of drug metabolites have to be taken into account when analysing PXR-dependent induction of drug metabolism and transport. The drug interaction potential of the active metabolite, *para*-hydroxy atorvastatin, might be lower than that of the parent compound.

Abbreviations

AD, activation domain; ADME, absorption distribution metabolism excretion; CAR, constitutive androstane receptor; CITCO, 6-(4-chlorophenyl)imidazo[2,1-*b*]thiazole-5-carbaldehyde *O*-(3,4-dichlorobenzyl) oxime; CYP, cytochrome P450; DBD, DNA-binding domain; DMSO, dimethyl sulphoxide; DRIP205, vitamin D receptor interacting protein 205; HMGCR, 3-hydroxy-3-methylglutaryl-coenzyme A reductase; kb, kilobase pair(s); LBD, ligand-binding domain; LDL, low-density lipoprotein; PXR, pregnane X receptor; RID, receptor interaction domain; SMRT, silencing mediator for retinoid and thyroid receptors; SRC-1, steroid receptor co-activator 1; TIF-2, transcriptional intermediary factor 2; UGT, UDP-glucuronosyltransferase

Introduction

Statins are widely used in the treatment of hypercholesterolaemia, which is a key feature of the metabolic syndrome in humans and an important risk factor for the development of cardiovascular diseases, such as myocardial infarction. By competitive inhibition of 3-hydroxy-3-methylglutaryl-coenzyme A reductase (HMGCR), the rate-limiting enzyme in cholesterol synthesis, statins cause the intracellular depletion of cholesterol, thereby inducing the proteolytic activation of sterol response element-binding proteins, which stimulates the expression of the low-density lipoprotein (LDL) receptor (Horton *et al.*, 2002). As one consequence, the plasma concentration of LDL cholesterol is lowered by increased hepatocellular uptake (Poli, 2007).

Atorvastatin has been prescribed for many years and is considered as one of the most potent agents within the statin drug class, in terms of the LDL cholesterol-lowering effect (Poli, 2007). However, the therapeutic response at a given dose is highly variable between individuals (Pedro-Botet *et al.*, 2001), and the correlation between plasma concentrations and response to atorvastatin is poor (Lennernäs, 2003). One reason may be the extensive first-pass metabolism and the consequent metabolism-dependent interconversion of active and inactive metabolites of atorvastatin (Figure 1). Conversion of the active acid form to the inactive lactone mainly requires an acylglucuronide intermediate (Prueksaritanont *et al.*, 2002), which is predominantly catalysed by UDP glucuronosyltransferase (UGT) 1A3 (Riedmaier *et al.*, 2010). Metabolism of the drug by cytochrome P450 (CYP)

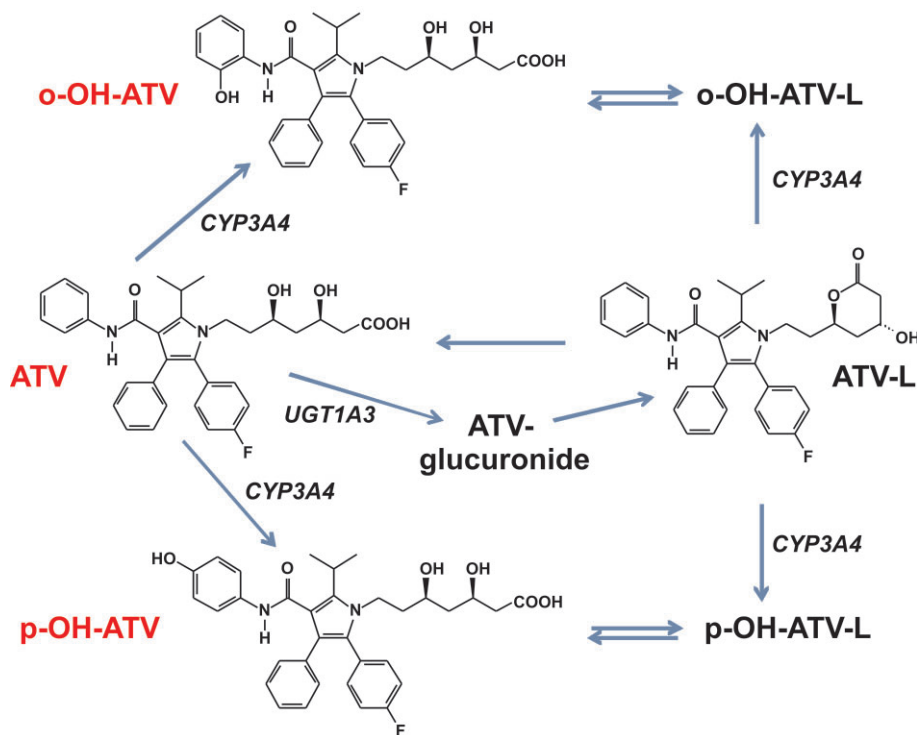


Figure 1

Chemical structures and metabolic pathways of atorvastatin and metabolites. Only the chemical structures of metabolites used in this study are shown. Metabolic pathways are displayed according to Jacobsen *et al.* (2000) and Prueksaritanont *et al.* (2002). ATV, atorvastatin; ATV-L, atorvastatin lactone, o-OH-ATV, *ortho*-hydroxy atorvastatin; p-OH-ATV, *para*-hydroxy atorvastatin.

3A4 results in the formation of the two active metabolites *ortho*-hydroxy and *para*-hydroxy atorvastatin (Jacobsen *et al.*, 2000). These two active metabolites are said to be responsible for the atorvastatin-related prolonged inhibition of HMGCR and the higher efficacy in lowering LDL cholesterol, as compared with other statins (Poli, 2007).

Disposition of a drug is also strongly influenced by transport processes. Hepatocellular uptake of atorvastatin, which is a substrate of the transporter SLCO1B1 (OATP1B1) (Kameyama *et al.*, 2005), is largely mediated by this membrane transport protein. For instance, atorvastatin pharmacokinetics is significantly altered by OATP1B1 inhibitors in humans (Lau *et al.*, 2007), as well as by SLCO1B1 genetic variants as shown by two independent studies (Pasanen *et al.*, 2007; Lee *et al.*, 2010). Moreover, atorvastatin is also a substrate of the efflux transporter ABCB1 (MDR1/P-glycoprotein) (Wu *et al.*, 2000; Hochman *et al.*, 2004), which influences pharmacokinetics of atorvastatin (Keskitalo *et al.*, 2008). Thus, multiple drug interactions because of the competitive inhibition of enzymes and/or transporters are conceivable and have been reported in the literature (see Lennernäs, 2003).

Additionally, atorvastatin, in common with many statins, induces the hepatic expression of CYP3A4 and CYP2B6 (Kocarek *et al.*, 2002), which suggests activation of the pregnane X receptor (PXR, NR1I2) and/or the constitutive androstane receptor (CAR, NR1I3; receptor nomenclature follows Alexander *et al.*, 2011). These two receptors are the main xenosensors in the body and are responsible for the adaptive response to xenobiotics, including drugs, by inducing the expression of drug-metabolizing enzymes and transporters. Especially, PXR is activated by a large spectrum of structurally diverse chemicals, which bind to the receptor as ligands (di Masi *et al.*, 2009). In contrast, the majority of CAR activators act by promoting the translocation of the receptor from the cytosol to the nucleus by an indirect mechanism, which is only partially understood and not involving ligand binding (Li and Wang, 2010). Thus, induction via activation of PXR and/or CAR may further contribute to atorvastatin-dependent drug interaction.

Given the extensive metabolism of atorvastatin and the contribution of the active metabolites, *ortho*-hydroxy and *para*-hydroxy atorvastatin, to the drug's therapeutic effect, it is important to consider their respective effects on drug interaction. Whereas the inhibition of drug-metabolizing enzymes and transporters by atorvastatin metabolites has been already studied (Chen *et al.*, 2005; Sakaeda *et al.*, 2006), an analysis regarding the induction of absorption distribution metabolism excretion (ADME) genes via PXR and/or CAR activation is still missing. Thus, the objective of the present study was to characterize atorvastatin, its lactone form, as well as both active hydroxy metabolites with respect to activation of PXR and/or CAR and subsequent induction of the corresponding target genes.

Here, we show that atorvastatin and its metabolites are ligands of PXR, but not of CAR. Interestingly, only the *para*-hydroxy metabolite showed significantly impaired induction of PXR-regulated genes, which may be explained by the impaired release of co-repressors from PXR by the metabolite. We conclude that the active metabolite, *para*-hydroxy atorvastatin, might have a reduced capacity to interact with other drugs.

Methods

Cell culture and generation of stable transfectants

The human hepatoblastoma cell line HepG2 was obtained from ATCC (Manassas, VA, USA) and grown in minimal essential medium, supplemented with 10% fetal calf serum, 2 mM L-glutamine, 100 U·mL⁻¹ penicillin and 100 U·mL⁻¹ streptomycin. A pool of cells stably expressing human PXR (HepG2-PXR) was generated by selection with 800 µg·mL⁻¹ G-418 sulphate of HepG2 cells, which were transfected with the expression plasmid pNTAP-huPXR by calcium phosphate co-precipitation as described by Geick *et al.* (2001), and further propagated in the presence of 200 µg·mL⁻¹ G-418. Expression of human PXR protein in HepG2-PXR cells was confirmed by Western blotting using the PXR-specific antibody N16. COS1 cells were cultivated in Dulbecco's modified Eagle's medium buffered with 25 mM HEPES, supplemented with 100 U·mL⁻¹ penicillin, 100 U·mL⁻¹ streptomycin, 2 mM L-glutamine, and 10% fetal calf serum.

Transient transfections, mammalian two-hybrid and reporter gene assays

One day before transfection, HepG2 or HepG2-PXR cells were plated in 24-well plates at a density of 1.5×10^5 cells per well, whereas COS1 cells were plated at a density of 3×10^4 cells per well. Transfections were performed using Effectene™ transfection reagent (QIAGEN, Hilden, Germany), according to the manufacturer's recommendations. For two-hybrid PXR assembly assays HepG2 cells were transfected with 150 ng of the reporter gene plasmid pGL3-G5, 20 ng of the expression plasmid encoding GAL4-DBD/PXR(132–188) and 10 ng of the expression plasmid encoding VP16-AD/PXR(189–434) per well. Two-hybrid CAR assembly assays were performed in COS1 cells as described previously (Burk *et al.*, 2005). For CYP3A4 promoter reporter gene assays, HepG2-PXR cells were transfected with 150 ng of the reporter gene plasmid pGL3-CYP3A4(-7830/Δ7208–364). Two-hybrid assays for the analysis of PXR interactions with co-activator or co-repressor were performed as described previously (Burk *et al.*, 2005). The β-galactosidase reference plasmid pCMVβ (20ng) was always co-transfected. If necessary, respective empty expression vectors or pUC18 were used to fill up to a total amount of 200 ng of plasmid DNA per well. Subsequently, cells were treated for 24 h or 40 h with the indicated drugs dissolved in dimethyl sulphoxide (DMSO) or with an equivalent amount of DMSO (final 0.1%). In case of treatment with statins for more than 24 h, 400 µM mevalonolactone was added to preserve normal cell growth. Luciferase and β-galactosidase activities were analysed as described previously (Burk *et al.*, 2002). Luciferase activity was normalized with respect to transfection efficiency using the corresponding β-galactosidase activity.

Bacterial protein expression and purification

Expression of soluble CAR-LBD and steroid receptor co-activator 1 (SRC-1)-RID His-tag fusion proteins was performed in *Escherichia coli* BL21(DE3), which were transformed with the respective bacterial expression plasmids and grown at 16°C for 20 h (CAR-LBD) or at 25°C for 4 h (SRC-1-RID) after induction of recombinant protein expression by 0.2 mM

isopropyl β -D-1-thiogalactopyranoside. Recombinant proteins were affinity purified using Talon His-tag purification resin (Clontech, Mountain View, CA, USA) and immediately diluted into the running buffer (see below). The purity of the eluted proteins was controlled by SDS-PAGE and silver staining of the protein gel.

Surface plasmon resonance

Measurement of protein–protein interaction was performed by surface plasmon resonance using the Biacore 3000 instrument (Biacore/GE Healthcare, Freiburg, Germany). All buffers were degassed before use. The receptor interaction domain of the steroid receptor co-activator 1 (SRC-1-RID) protein was diluted into 10 mM sodium acetate pH 5 and immobilized on the dextrane matrix of a CM5 sensor chip using amine coupling. A reference cell was used to subtract possible non-specific binding of CAR-LBD protein to the chip surface. Running buffer consisted of 50 mM sodium phosphate pH 7.5, 150 mM sodium chloride, 0.1% Tween 20, 1 mM β -mercaptoethanol and 1% DMSO. Assays were performed at 25°C using a flow rate of 50 μ L·min⁻¹ to minimize mass transfer. Atorvastatin metabolites and 6-(4-chlorophenyl)imidazo[2,1-*b*]thiazole-5-carbaldehyde *O*-(3,4-dichlorobenzyl) oxime (CITCO) were prepared in DMSO as 30 mM and 100 mM stock solutions respectively. Compounds were diluted into running buffer to yield a final concentration of 100 μ M. Before each assay, the system was primed at least three times, and three injections of running buffer and regeneration solution, respectively, were performed to optimize baseline stability. Each assay contained at least three injections of running buffer, ligands only and a 1% DMSO solvent control. Before injection, each cycle was able to establish a stable baseline for at least 90 s. CAR-LBD protein (0.21 μ M) was injected either alone to define the constitutive binding to the immobilized co-activator or after an incubation of at least 30 min with the compounds at room temperature. Both association and dissociation were measured for 1 min. The post-dissociation phase comprised two-step regeneration and an extra clean washing step with running buffer. The first regeneration solution consisted of 10 mM sodium hydroxide, 150 mM sodium chloride and 0.03% SDS, whereas the second was made up by normal running buffer.

Primary human hepatocytes

Experimental procedures complied with the Guidelines of the charitable state-controlled Foundation for Human Tissue and Cell Research (Thasler *et al.*, 2003), the respective institutional guidelines and were approved by the local ethical committees of the Ludwig-Maximilians-University of Munich, the University Medical Centre Regensburg and the Charité, Humboldt University Berlin, Germany. Tissue samples from human liver resections were obtained, with full consent, from patients undergoing partial hepatectomy because of primary or secondary liver tumours. Detail of the donors are given in Supporting Information Table S1. Human hepatocytes were isolated from the samples using a modified two-step EGTA/collagenase perfusion procedure as described previously (Weiss *et al.*, 2003; Nussler *et al.*, 2009). Viability of isolated hepatocytes was determined by Trypan blue exclusion. Only

cell preparations with a viability >80% were used for experiments. The isolated cells were seeded at a density of 1.5×10^6 cells per well into collagen type I-coated six-well plates and cultivated at 37°C in a humidified incubator with 5% CO₂ in Williams' E medium, supplemented with 10% fetal calf serum, 15 mM HEPES, 0.1 mM non-essential amino acids, 1 mM sodium pyruvate, 2 mM L-glutamine, 100 U·mL⁻¹ each of penicillin and streptomycin, 0.032 IU·mL⁻¹ insulin and 100 nM dexamethasone. After 2 days, cultures were maintained for 24 h in serum-free Williams' E medium supplemented with 2 mM L-glutamine, 100 nM dexamethasone, 1% insulin-transferrin-selenium-G (ITS-G), and 100 U·mL⁻¹ each of penicillin and streptomycin. Thereafter, cells were treated for 48 h with the indicated chemicals or with an equivalent amount (final 0.1%) of DMSO only. As shown in Supporting Information Figure S1, these cultures of human hepatocytes, as described above, generally maintained the expression of xenosensor PXR and co-activator SRC-1, whereas expression of co-repressor silencing mediator for retinoid and thyroid receptors (SMRT) was increased compared with matched, freshly isolated cells. CYP3A4 and CYP2B6 expression were down-regulated to at most 25% and <10% respectively. Thus, these culture conditions were suitable for induction studies.

Quantitative real-time PCR analysis

Total RNA and first-strand cDNA were prepared as previously described (Burk *et al.*, 2002). The integrity of RNA samples was confirmed by formaldehyde agarose gel electrophoresis. Only the samples that showed sharp ribosomal RNA bands (28S twice as intense as 18S) and did not show any visible signs of degradation, were further processed. PCR reactions were set up with cDNA corresponding to 25 pg (18S rRNA) or 25 ng (all other assays) of total RNA and the qPCR MasterMix Plus Low ROX (Eurogentec, Seraing, Belgium). Gene expression levels were quantified by TaqMan real-time quantitative PCR using the 7500 Real-Time PCR System (Applied Biosystems, Foster City, CA, USA). The experiments were performed in a final volume of 25 μ L using the default settings of the 7500 Real-Time PCR system. Assays were done in triplicate. Oligonucleotide primers and probes, designed with Primer-Express software version 2.0 (Applied Biosystems), are shown in Supporting Information Table S2. The TaqMan gene expression assays Hs00168352_m1 and Hs00196955_m1 (Applied Biosystems) were used for the quantification of HMGCR and SMRT mRNA expression respectively. Serial dilutions of respective linearized cDNA plasmids were used to create the calibration curves, ranging from 30 to 3×10^7 copies. The respective gene expression levels were normalized to the corresponding 18S rRNA level and calculated as copies per 10⁸ copies of 18S rRNA.

Protein analysis

Hepatocytes were scraped off the plate using ice-cold PBS. Cells were lysed by 30 min incubation on ice in 50 mM Tris-Cl pH 8.0, 150 mM NaCl, 1 mM EDTA, 1% (v/v) Nonidet P-40, supplemented with 1 \times Halt protease inhibitor cocktail. Total protein lysates were quantified using the bicinchoninic acid method and a calibration curve generated with serial dilutions of BSA. Samples (30 μ g protein) of each lysate were

separated on a 10% SDS-polyacrylamide gel and transferred to nitrocellulose membrane by electroblotting. Transfer was controlled by Ponceau S staining. Blots were sequentially incubated with primary antibodies specific for CYP2B6, CYP3A4 and β -actin, each followed by incubation with the respective secondary peroxidase-conjugated antibody and detection by means of chemiluminescence using substrate SuperSignal West Dura. Protein bands were quantified with Fuji LAS-1000 CCD camera (Raytest, Straubenhardt, Germany) and AIDA software (Raytest).

Data analysis and statistical procedures

For transient transfections, the mean values of at least three independent experiments, each performed in triplicate, were used for statistical analysis. Multiple comparisons were generally performed using one-way ANOVA with post tests, as indicated in the respective figure legends. To concurrently analyse the effect of treatment with chemicals and co-transfections of co-factors, two-way ANOVA with Bonferroni's post-test was used (see Figure 6). Comparisons to a hypothetical mean were performed using one sample *t*-test, and the resulting *P*-values were corrected for multiple testing by the method of Bonferroni.

As hepatocyte mRNA expression data were not normally distributed, multiple comparisons were performed using Kruskal–Wallis test or Friedman test with Dunn's multiple comparisons post-test, whereas comparisons to a hypothetical mean were performed using Wilcoxon signed rank test. Pairwise comparisons of CYP protein induction data in hepatocytes were performed using the paired *t*-test.

All calculations were done using GraphPad Prism 5.04 or InStat 3.10 (GraphPad Software, La Jolla, CA, USA). Statistical significance was defined as *P* < 0.05.

Plasmids

All plasmids used in transient transfection analyses have been described previously: human CYP3A4 enhancer/promoter reporter gene plasmid pGL3-CYP3A4(-7830/ Δ 7208–364) (Hustert *et al.*, 2001); the Gal4-dependent reporter gene construct pGL3-G5 and the expression plasmids encoding fusion proteins of the GAL4 DNA-binding domain (DBD) and receptor interaction domains (RID) of human co-activators SRC-1 (NCOA1, amino acids 583–783), transcriptional intermediary factor (TIF-2; NCOA2, amino acids 583–779) and vitamin D receptor interacting protein 205 (DRIP205; MED1, amino acids 527–774) (Arnold *et al.*, 2004); expression plasmids encoding fusion proteins of the VP16-activation domain (AD) and human PXR or CAR ligand-binding domain (LBD) or parts of it (PXR amino acids 108–434, 189–434; CAR amino acids 151–348), expression plasmids encoding fusion proteins of the GAL4-DBD and the helix 1 parts of human PXR or CAR-LBD (PXR amino acids 132–188; CAR amino acids 105–150) and the expression plasmid encoding a fusion protein of the GAL4-DBD and RID of human co-repressor SMRT (NCOR2, amino acids 1109–1330) (Burk *et al.*, 2005). The β -galactosidase expression plasmid pCMV β was purchased from Clontech.

The expression plasmid pNTAP-huPXR was constructed by cloning the open reading frame of human PXR, amplified by PCR out of pcDhPXR (Geick *et al.*, 2001) using primers

5'-AGT GGA TCC ATG GAG GTG AGA CCC AAA GAA AGC -3' and 5'-GAT GAA TTC TCA GCT ACC TGT GAT GCC GAA CAA -3'. The oligonucleotides introduced BamHI and EcoRI restriction sites at the 5'- and 3'-ends of the amplified fragment respectively. The BamHI/EcoRI digested PCR fragment was cloned into appropriately digested vector pNTAP-B (Stratagene, La Jolla, CA, USA).

Bacterial expression plasmids encoding the LBD (amino acids 105–348) of human CAR or the RID (amino acids 583–783) of human SRC-1 were constructed by cloning PCR-amplified appropriate DNA fragments into pET-28a(+) or pET-22b(+) vector (Novagen/Merck Biosciences, Darmstadt, Germany) respectively. The PCR-amplified SRC-1 fragment additionally contains a sequence encoding N-terminal 10xHis-tag in frame with the SRC-1 part and a downstream stop codon. Thus, both bacterial expression plasmids encode the respective proteins as N-terminal His-tag fusions. The identities of all PCR-amplified DNA fragments were verified by sequencing.

Materials

Atorvastatin, atorvastatin lactone, *ortho*-hydroxy atorvastatin, and *para*-hydroxy atorvastatin were purchased from Toronto Research Chemicals (North York, Canada). DMSO (+/-)-mevalonolactone, rifampin, phenobarbital, clofibrate, triphenylphosphate, clotrimazole, PK11195, pravastatin and dexamethasone were purchased from Sigma-Aldrich (Taufkirchen, Germany). CITCO and G418-sulphate were purchased from BIOMOL/Enzo Life Sciences (Plymouth Meeting, PA, USA) and Calbiochem/Merck Biosciences (Darmstadt, Germany) respectively.

The following cell culture reagents were purchased from Invitrogen (Carlsbad, CA, USA): minimal essential medium, Williams' E medium, non-essential amino acids, sodium pyruvate and ITS-G supplement. Fetal calf serum was obtained from Sigma-Aldrich, whereas Dulbecco's modified Eagle's medium buffered with 25 mM HEPES, L-glutamine and penicillin–streptomycin solution were purchased from BioWhittaker/Lonza (Verviers, Belgium). Twenty-four-well cell culture plates were obtained from BD Biosciences Discovery Labware (Bedford, MA, USA).

Antibodies used in immunoblotting were obtained as follows: PXR-specific antibody N16 (sc-9690) from Santa Cruz (Santa Cruz, CA, USA), antibodies WB-3A4 and INHIBITION MAB-2B6, specific for CYP3A4 and CYP2B6, respectively, from BD Biosciences (Heidelberg, Germany), the β -actin antibody (clone AC-15) from Sigma-Aldrich and the respective secondary peroxidase-conjugated antibodies from Dako (Glostrup, Denmark).

Further reagents were purchased as indicated: Effectene transfection reagent from QIAGEN, Talon His-tag purification resin from Clontech, PageSilver silver staining kit from Fermentas (Sankt Leon-Rot, Germany), sensor chip CM5 and amine coupling kit from Biacore/GE Healthcare, qPCR Master-Mix Plus Low ROX from Eurogentec, Halt protease inhibitor cocktail and SuperSignal West Dura chemiluminescent substrate from Thermo Scientific/Pierce (Rockford, IL, USA). Oligonucleotide primers and TaqMan probes were custom-synthesized by Biomers (Ulm, Germany) and Applied Biosystems respectively.

Results

Atorvastatin and its metabolites are ligands of human PXR and induce PXR-dependent CYP3A4 promoter activity

Atorvastatin has been shown to induce CYP3A4 and CYP2B6 gene expression in primary human hepatocytes (Kocarek *et al.*, 2002), thereby suggesting activation of PXR and/or CAR. However, the respective molecular mechanism has not yet been fully elucidated, as much as the role of atorvastatin lactone and hydroxy metabolites in the induction of CYP expression has not been addressed. To analyse whether atorvastatin and/or its metabolites are ligands of PXR, we applied a previously developed assembly assay, relying on the ligand-dependent interaction of fragments of the PXR-LBD (Burk *et al.*, 2005). Figure 2A shows that rifampin, a well-known prototypical ligand of human PXR, efficiently induced the interaction of PXR helix 1 with the remainder of the LBD. Similarly, atorvastatin lactone and both hydroxy metabolites also induced PXR-LBD assembly, however, weaker than rifampin, whereas the parent compound showed only a marginal effect. Among all the metabolites, atorvastatin lactone was the most potent inducer of PXR-LBD assembly.

Next, we asked whether atorvastatin and its metabolites may act as PXR agonists because antagonists also induce the assembly of nuclear receptor helix 1 fragments with the remainder of the LBD (Pissios *et al.*, 2000 and data not shown). Figure 2B clearly shows that all of them induced the PXR-dependent transactivation of the CYP3A4 enhancer/promoter reporter gene in transiently transfected HepG2-PXR cells. The parent compound and the *para*-hydroxy metabolite showed significantly reduced activity, whereas the lactone and the *ortho*-hydroxy metabolite induced PXR-activity similar to rifampin. Dose-response analysis further revealed that rifampin activated PXR with an EC₅₀ value of 1.8 μM (95% CI 1–4 μM), whereas atorvastatin lactone exhibited an EC₅₀ value of >8 μM, which could not be determined more

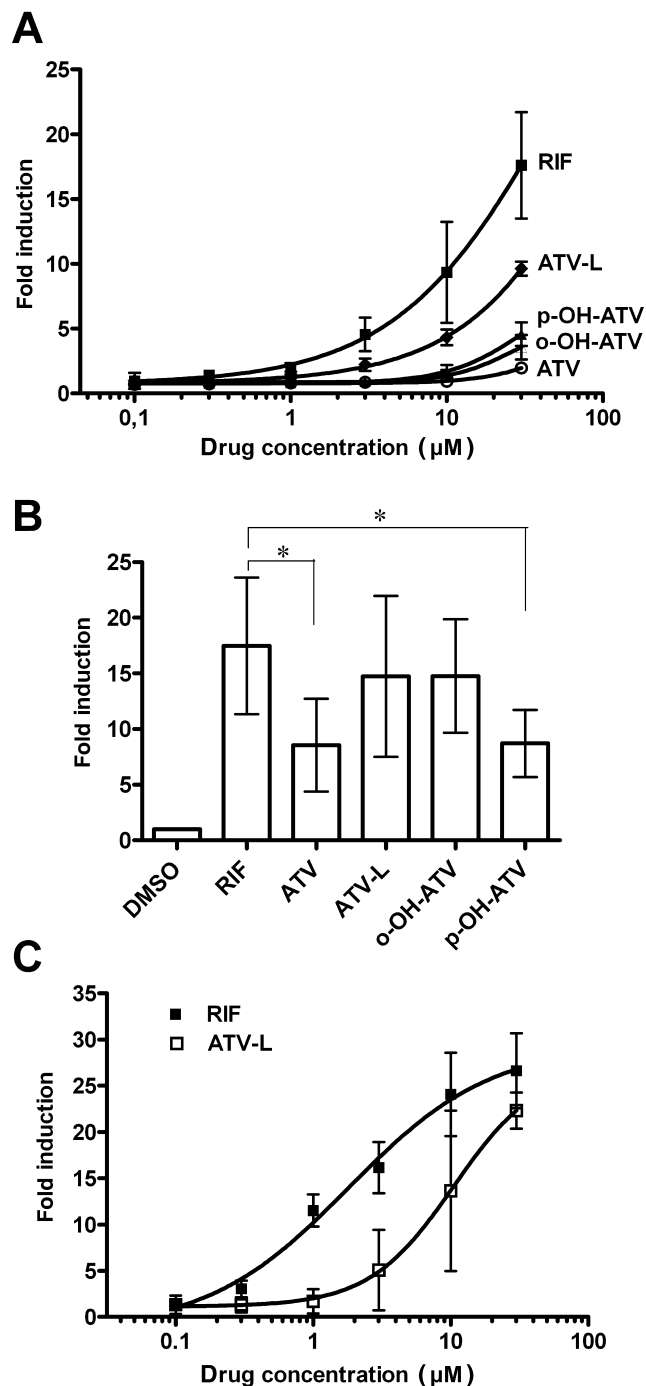
Figure 2

Atorvastatin and its metabolites induce assembly of the human PXR-LBD and CYP3A4 promoter activity. (A) PXR-assembly assay in HepG2 cells, co-transfected with expression plasmids encoding GAL4-DBD/hPXR-LBD (132–188) and VP16-AD/hPXR-LBD (189–434) fusion proteins. Cells were treated for 40 h with 0.1% DMSO or increasing concentrations of the indicated compounds. Mean fold induction (±SD) of the respective normalized activity of co-transfected reporter plasmid pGL3-G5 by treatment with the indicated concentrations of compounds is shown. (B) and (C) HepG2-PXR cells were transfected with pGL3-CYP3A4(-7830/Δ7208–364) and treated with increasing concentrations (C) or with 30 μM of the indicated compounds (B) for 24 h. The columns (B) and graphs (C) show mean fold induction (±SD) of normalized CYP3A4 promoter reporter gene activity by treatment with compounds. The respective reporter activity of transfected cells, which were treated with DMSO only, was designated as 1. Data were analysed by repeated measures one-way ANOVA with Bonferroni's multiple comparisons post-test. **P* < 0.05, significant differences between groups as shown. RIF, rifampin; ATV, atorvastatin; ATV-L, atorvastatin lactone, *o*-OH-ATV, *ortho*-hydroxy atorvastatin; *p*-OH-ATV, *para*-hydroxy atorvastatin.

precisely as the activation plateau was not reached by 30 μM (Figure 2C).

Atorvastatin and its metabolites do not bind to human CAR as ligands

By applying our previously described cellular assembly assay for human CAR (Burk *et al.*, 2005), we analysed whether atorvastatin and its metabolites may bind to CAR as ligands. Figure 3A shows that they did not induce the assembly of the human CAR-LBD, in clear contrast to CITCO, a well-known ligand for human CAR. The suitability of this assay for the



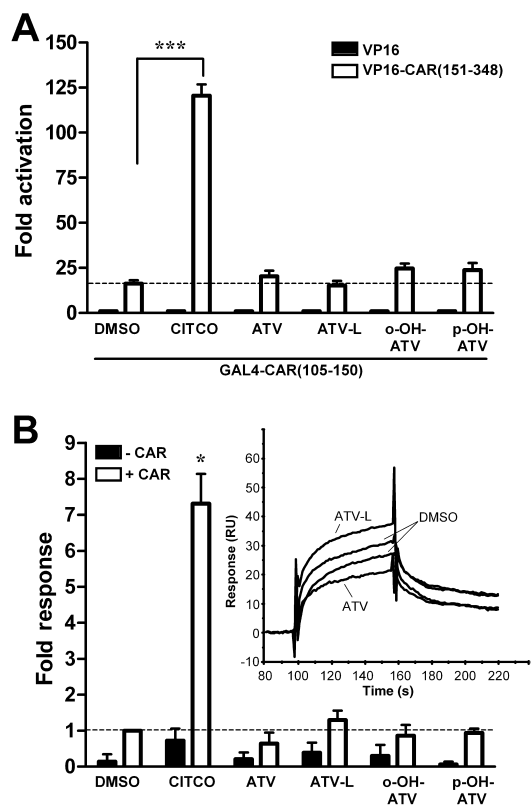


Figure 3

Atorvastatin and its metabolites neither induce the assembly of CAR-LBD nor the *in vitro* interaction with co-activator SRC-1. (A) CAR assembly assay in COS1 cells, which were co-transfected with expression plasmids encoding GAL4-DBD/hCAR-LBD (105–150) and VP16-AD/hCAR-LBD (151–348) fusion proteins (open columns) or empty expression vector pVP16-AD (filled columns). Cells were treated for 40 h with 1 μ M CITCO, 30 μ M of atorvastatin or metabolites or 0.1% DMSO only. Mean fold activation (\pm SD) of the normalized activity of co-transfected reporter plasmid pGL3-G5 by treatment with the indicated compounds is shown. The respective activity of cells transfected with GAL4-DBD/hCAR-LBD(105–150) expression plasmid and pVP16-AD, treated with DMSO only, was designated as 1. Data were analysed by one-way ANOVA with the Tukey-Kramer post-test. *** P < 0.001, significant effect of CITCO. (B) Biacore analysis of ligand-induced interaction of co-activator SRC-1 with CAR *in vitro*. CAR-LBD protein, pre-incubated with 10 μ M CITCO or 100 μ M of the indicated atorvastatin metabolites or 1% DMSO only, was injected onto immobilized SRC-1-RID protein (+CAR). As a control, compounds were also injected alone (-CAR). Data are shown as means \pm SD of four to six independent experiments. Open columns show increase in binding by pre-incubation of CAR with compounds. Binding of CAR to SRC-1 in the presence of DMSO only, was designated as 1. Data were analysed by one sample *t*-test and *P*-values corrected for multiple testing by the method of Bonferroni, * P < 0.05, significant effect of CITCO. The inset shows representative individual sensorgrams of CAR pre-incubated with ATV, ATV-L or vehicle DMSO only. ATV, atorvastatin; ATV-L, atorvastatin lactone, o-OH-ATV, *ortho*-hydroxy atorvastatin; p-OH-ATV, *para*-hydroxy atorvastatin.

identification of CAR ligands, whether agonists or inverse agonists, is shown in Supporting Information Figure S2A. Further cellular two-hybrid co-activator interaction assays using co-activators SRC-1 or TIF-2 together with reference

variant CAR (Supporting Information Figure S3A,B) or using co-activator DRIP205 with the ligand-dependent CAR-SV2 splice variant (Arnold *et al.*, 2004) (Supporting Information Figure S3C) confirmed that atorvastatin and its metabolites did not change human CAR activity by ligand binding. These compounds also did not change the interaction of CAR with co-repressor SMRT in a cellular two-hybrid assay (Supporting Information Figure S3D). Additionally, we established an *in vitro* Biacore protein–protein interaction assay using bacterially expressed human CAR-LBD and co-activator SRC-1-RID proteins. Treatment with CITCO clearly increased the binding of CAR to SRC-1, whereas atorvastatin and its metabolites did not show any significant effect (Figure 3B). Further negative and positive controls for the *in vitro* Biacore interaction assay are shown in Supporting Information Figure S2B.

Atorvastatin and its metabolites differentially induce the hepatic expression of PXR-regulated genes

Having shown that atorvastatin and its metabolites are ligands only for human PXR, we assessed their respective induction capacity using primary human hepatocytes and the induction of endogenous CYP3A4 and UGT1A3 expression, as measured by quantitative real-time PCR. Treatment with the prototypical PXR ligand rifampin induced CYP3A4 mRNA expression with median 8.6-fold (range: 4.7–16.3). Atorvastatin, atorvastatin lactone and *ortho*-hydroxy atorvastatin all induced CYP3A4 expression to a similar extent, with medians (range) of 6.5- (3.1–12.7), 7.1- (3.9–12.3) and 7.9- (1.8–12.7) fold respectively. In contrast, induction of CYP3A4 by *para*-hydroxy atorvastatin was significantly reduced, with median 2.5-fold, ranging from 0.4- to 4.4-fold in individual cultures. As expected (Kocarek *et al.*, 2002) and thus used as a negative control, pravastatin did not induce CYP3A4 expression at all (Figure 4A). Regarding UGT1A3 expression, Figure 4B shows that this gene was induced with similar median fold changes by rifampin, atorvastatin and its metabolites. To prove the successful inhibition of cholesterol biosynthesis, which has to result in the compensatory increased expression of HMGCR (Horton *et al.*, 2002), we further analysed HMGCR mRNA expression in the drug-treated hepatocytes. HMGCR expression showed the expected increase in cultures, which were treated with the pharmacologically active atorvastatin (median 10.0-fold, range 6.5–12.3), *ortho*-hydroxy atorvastatin (median 8.0-fold, range 4.2–9.8), and *para*-hydroxy atorvastatin (median 8.4-fold, range 5.2–15.3), but also demonstrated an increase in cultures treated with the inactive atorvastatin lactone (median 8.6-fold, range 4.4–9.5) (Figure 4C), which can only be explained by substantial conversion of the lactone to the acid form in human hepatocytes. As expected, HMGCR gene expression was not induced by rifampin (Figure 4C).

Having shown the differential impact of the two hydroxy metabolites of atorvastatin on the expression of CYP3A4 and UGT1A3, we investigated their effect on the expression of other genes, known to be regulated by PXR. Figure 5A–D shows that rifampin and the *ortho*-hydroxy metabolite both significantly induced the expression of CYP2B6, EPHX1, ABCB1 and SLCO1B1, compared with treatment with DMSO only (P < 0.05, Wilcoxon signed rank test). In contrast,

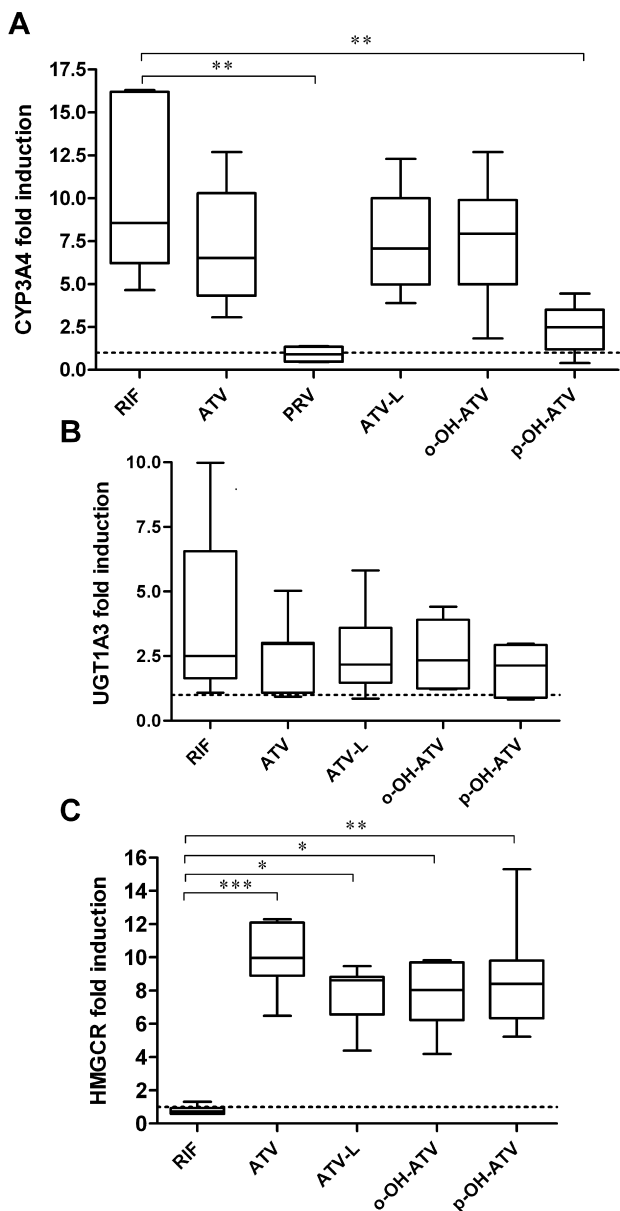


Figure 4

Atorvastatin and its metabolites differentially induce hepatic gene expression in primary human hepatocytes. Primary human hepatocyte cultures ($n = 7$, PRV $n = 4$) were treated with 30 μM of the indicated chemicals or 0.1% DMSO only. After 48 h of treatment total RNA was prepared, followed by analysis of CYP3A4 (A), UGT1A3 (B) and HMGCR (C) mRNA expression by TaqMan real-time RT-PCR. Expression levels were normalized with respect to the corresponding expression of 18S rRNA. Data are shown as fold induction by treatment with chemicals as compared with the treatment with DMSO only, which was designated as 1, and are presented as box and whisker plots, with boxes representing the 25th–75th percentiles, medians indicated by horizontal lines and whiskers showing minimum and maximum values. Data were analysed by Kruskal–Wallis test with Dunn’s multiple comparisons post-test. *** $P < 0.001$, ** $P < 0.01$, * $P < 0.05$, significant differences between groups as shown. RIF, rifampin; ATV, atorvastatin; ATV-L, atorvastatin lactone, o-OH-ATV, *ortho*-hydroxy atorvastatin; p-OH-ATV, *para*-hydroxy atorvastatin; PRV, pravastatin.

the *para*-hydroxy metabolite only weakly induced ABCB1 ($P < 0.05$, Wilcoxon signed rank test).

Impaired induction of CYP3A4 and CYP2B6 genes by *para*-hydroxy atorvastatin is manifested on the protein level

Induction of CYP and ABCB1 genes is functionally relevant, as it results in elevated protein levels, which influence the pharmacokinetics of drug substrates. Using hepatocytes from three additional donors, we assayed the protein levels of CYP3A4, CYP2B6 and ABCB1, after treatment with the hydroxy atorvastatin metabolites. Figure 6 shows that CYP3A4 and CYP2B6 proteins were induced by *ortho*-hydroxy atorvastatin and rifampin, to a similar extent. Mean induction of CYP3A4 protein by *para*-hydroxy atorvastatin was significantly reduced by 40% ($P = 0.0017$, paired *t*-test), compared with the *ortho*-hydroxy metabolite. A similar trend, however, not reaching significance, was observed for CYP2B6 protein ($P = 0.0712$, paired *t*-test). The MDR1/P-glycoprotein, which is encoded by the ABCB1 gene, was induced by rifampin but there was no consistent induction by the two hydroxy metabolites of atorvastatin (data not shown). The difference in induction of CYP3A4 and CYP2B6 between the two metabolites is smaller, in terms of the protein than the corresponding mRNA (see Figures 4 and 5), which we also confirmed for these three hepatocyte cultures, by analysing mRNA induction, showing that expression of both CYP genes was approximately 3.5-fold higher by *ortho*-hydroxy atorvastatin than by the *para*-hydroxy metabolite.

Atorvastatin and its metabolites differentially modulate the interaction of co-regulatory proteins with human PXR

Having shown that the induction of some PXR target genes was strongly impaired in *para*-hydroxy atorvastatin-treated primary human hepatocytes, we attempted to elucidate the corresponding molecular mechanisms. In general, activation of nuclear receptors involves the ligand-dependent release of co-repressors and subsequent ligand-dependent interaction with co-activators. Thus, we performed mammalian two-hybrid assays that rely on the interaction of the PXR-LBD with RIDs of co-regulatory proteins. First, we analysed the ligand-dependent interaction with co-activators SRC-1 (NCOA1), TIF-2 (NCOA2) and DRIP205 (MED1), which are known to be recruited to PXR in a ligand-dependent manner. Atorvastatin only induced the interaction of PXR with SRC-1, whereas the lactone and both hydroxy metabolites stimulated the interaction of PXR with all three co-activators tested. However, the effect was not as pronounced as with the prototypical ligand rifampin (Figure 7A–C). Most importantly, significant differences in the interaction of PXR and co-activators were not observed between *ortho*-hydroxy and *para*-hydroxy atorvastatin treatment. Next, we analysed the ligand-dependent release of co-repressor SMRT (NCOR2). In the absence of ligands, the PXR-LBD constitutively interacted with this co-repressor. Rifampin, atorvastatin, atorvastatin lactone and *ortho*-hydroxy atorvastatin abolished this interaction. In contrast, *para*-hydroxy atorvastatin only produced a limited (50%) release of co-repressor SMRT (Figure 7D).

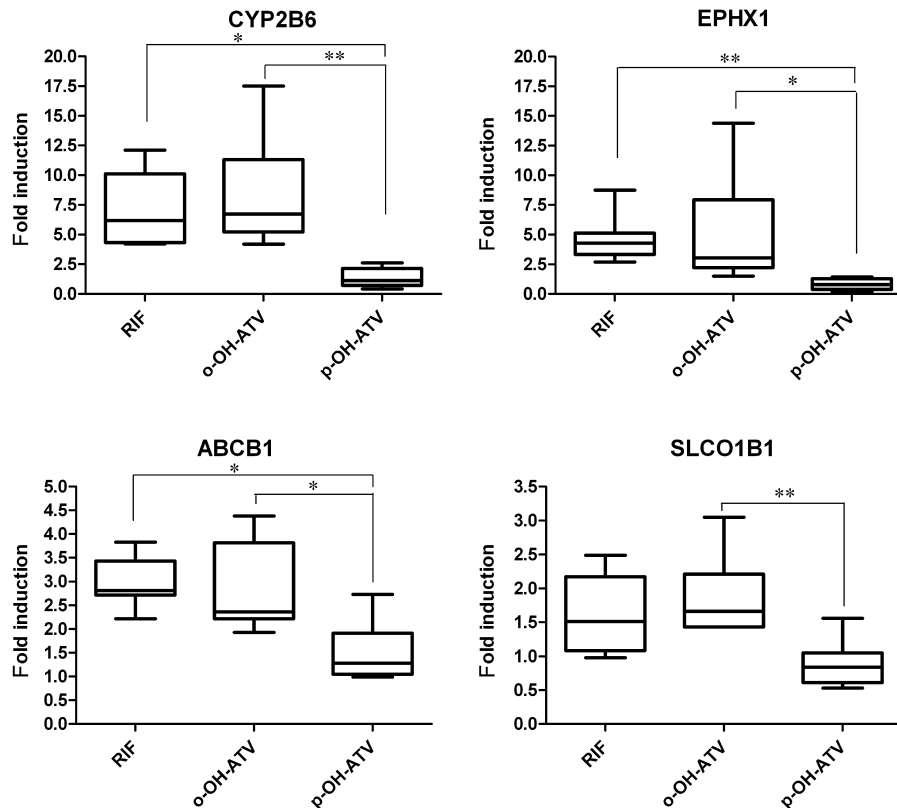


Figure 5

The hydroxy metabolites of atorvastatin differentially induce the expression of PXR target genes. Expression of CYP2B6, EPHX1, ABCB1 and SLCO1B1 was analysed by TaqMan real-time RT-PCR of the mRNA samples of primary human hepatocyte cultures, which were treated with rifampin (RIF), *ortho*-hydroxy atorvastatin (o-OH-ATV), *para*-hydroxy atorvastatin (p-OH-ATV) or DMSO (see legend of Figure 4). Fold induction by treatment with rifampin and the atorvastatin hydroxy metabolites was calculated with respect to expression levels by treatment with DMSO only, which was designated as 1. The data are presented as box and whisker plots as described in Figure 4. Data were analysed by Friedman's test with Dunn's multiple comparisons post-test. * $P < 0.05$, ** $P < 0.01$, significant differences between groups as shown.

Discussion and conclusions

Atorvastatin induces the expression of CYP2B6, CYP2C8, CYP2C9 and CYP3A4 mRNA, protein and enzymic activity in hepatocytes (Kocarek *et al.*, 2002; Feidt *et al.*, 2010) and activates human PXR and CAR in reporter gene assays (Kobayashi *et al.*, 2005; Monostory *et al.*, 2009; Yamasaki *et al.*, 2009), thereby suggesting ligand binding to these xenosensing nuclear receptors as the molecular mechanism of induction. It was the aim of this study to elucidate this hypothesis and to analyse any potential role of atorvastatin metabolites in induction.

Atorvastatin and its primary metabolites are ligands for human PXR but not for CAR. In the PXR assembly assay (Burk *et al.*, 2005), atorvastatin, both in its acid and lactone forms, and atorvastatin *ortho*- and *para*-hydroxy metabolites all were ligands of PXR. Nuclear receptor assembly assays, which rely on the ligand-dependent interaction of the respective LBD helix 1 fragment with the remainder of its LBD, reflect the intramolecular conformational change of helix 1 and subsequent stabilization of the LBD structure upon ligand binding (Pissios *et al.*, 2000). The usefulness of the PXR assembly assay

for the identification of ligands has recently been confirmed (Kobayashi *et al.*, 2010). In this assay, the lactone form of atorvastatin showed the highest potency; however, this does not necessarily reflect the highest binding affinity to PXR. Atorvastatin lactone is more lipophilic than the acid form and may simply enter cells more readily (Yamasaki *et al.*, 2009).

It was claimed that statins, including atorvastatin, are ligands of CAR (Willrich *et al.*, 2009), suggested by the activation of co-transfected CAR in hepatoma cell lines by statins, using CYP2B6 and CYP3A4 promoter reporter gene assays (Kobayashi *et al.*, 2005; Monostory *et al.*, 2009). However, very recent studies also using promoter reporter gene assays have questioned the activation of CAR by statins (Howe *et al.*, 2011; Omiecinski *et al.*, 2011). Using different cellular and *in vitro* assays, all relying on ligand-dependent protein-protein interactions as a measure of ligand binding, it is unequivocally shown that neither atorvastatin nor any of its metabolites act as ligands of reference variant human CAR or of the ligand-dependent splice variant CAR-SV2 (Arnold *et al.*, 2004). CAR-SV2 is said to account for approximately 40% of human CAR transcripts (Jinno *et al.*, 2004) and exhib-

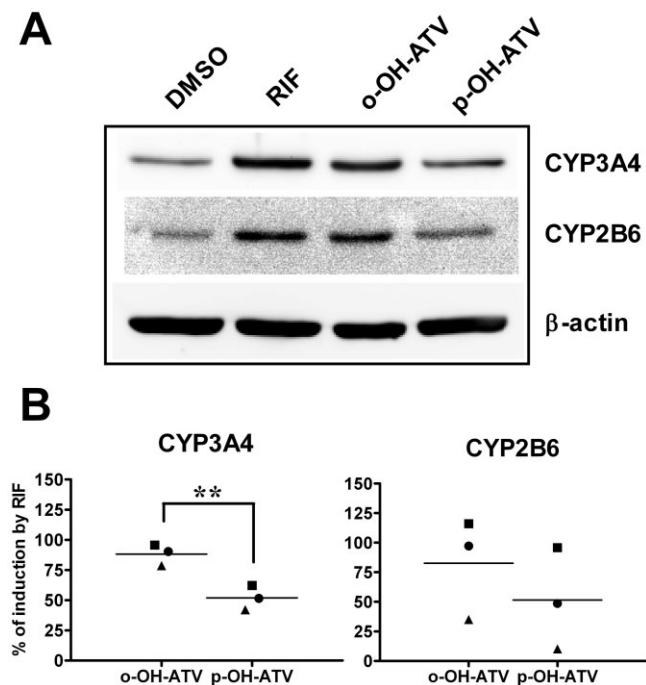


Figure 6

para-Hydroxy atorvastatin shows reduced induction of CYP protein expression. Primary human hepatocyte cultures ($n = 3$) were treated with 30 μM of the indicated chemicals or 0.1% DMSO only. After 48 h of treatment, total cellular protein lysates were prepared, followed by Western blot analysis of the indicated proteins. (A) Representative Western blot results from one individual culture. (B) Mean induction of CYP3A4 and CYP2B6 protein by *ortho*-hydroxy (*o*-OH-ATV) and *para*-hydroxy atorvastatin (*p*-OH-ATV) was calculated by normalizing CYP expression to β -actin and further comparing it with the extent of induction by rifampin (RIF), which was designated as 100%. Data were analysed by paired *t*-test. $**P < 0.01$, significant differences between groups as shown.

its specific ligand binding (Dring *et al.*, 2010). Treatment with atorvastatin activated AMP-activated kinase (Sun *et al.*, 2006), which was further demonstrated to be involved in the activation of CAR by phenobarbital-type activators and subsequent translocation of the receptor into the nucleus (Rencurel *et al.*, 2005; Shindo *et al.*, 2007). Thus, the discrepancy between the findings reported here and the previously published results (Kobayashi *et al.*, 2005; Monostory *et al.*, 2009), with respect to the activation of CAR by atorvastatin, may be explained by ligand-independent, phenobarbital-type activation of CAR in the cells used in these studies. Studies directly addressing nuclear translocation of CAR in hepatocytes by treatment with atorvastatin are clearly required to resolve the issue.

Atorvastatin induces a broader spectrum of ADME genes in hepatocytes than previously thought, now including phase II drug-metabolizing enzyme and drug transporter genes, besides the already known CYP genes. As SLCO1B1/OATP1B1 and ABCB1/P-glycoprotein mediate hepatic uptake and efflux of atorvastatin, respectively, and CYP3A4 and UGT1A3 are the main detoxifying enzymes, atorvastatin may induce all the steps of its own elimination. Autoinduction of

elimination may thus further contribute to the inter-individual variability in disposition and therapeutic efficacy of atorvastatin. However, induction of drug metabolism and transport by atorvastatin has, up to now, been demonstrated only in cell-based promoter reporter gene assays and in hepatocytes *ex vivo* (Marino *et al.*, 2011). Evidence for the mechanism to be active in liver *in vivo* is still missing, to the best of our knowledge, clearly asking for appropriately designed clinical studies, which may also address the autoinduction of elimination suggested here, by analysing the time dependency of the drug's pharmacokinetics with repeated dosing regimens.

Apart from the parent drug, the metabolites of atorvastatin also participate in the induction by PXR but not all are equally efficient as inducers. The *para*-hydroxy metabolite showed a significantly reduced induction of PXR target genes, except for UGT1A3, compared with the other metabolites. Because UGT1A3 was as well induced by both hydroxy metabolites, the difference seen in induction of the other genes is most likely not to be the consequence of altered metabolism or transport of *para*-hydroxy atorvastatin in hepatocytes. *para*-Hydroxy atorvastatin also induced HMGCR expression as strong as the other compounds, indicating that it is efficiently taken up into cells. This conclusion is further supported by studies reporting that both hydroxy metabolites are equally well transported by OATP1B1 (Lau *et al.*, 2007). Similarly, as the PXR assembly and co-activator interaction assays did not show weaker activity of the *para*-hydroxy as compared with the *ortho*-hydroxy metabolite, differences in ligand binding affinity and co-activator recruitment most likely do not account for the impaired induction capacity of *para*-hydroxy atorvastatin. However, this metabolite showed less co-repressor release, which suggests the molecular mechanism of its impaired induction capacity in hepatocytes (Figure 8). In the absence of an agonist, PXR is bound to co-repressors, as, for example, SMRT, resulting in inactive receptor complexes. Upon agonist binding, conformation of the receptor is changed, the co-repressors dissociate and co-activators, as, for example, SRC-1, are recruited to the receptor, resulting in active receptor complexes and subsequently in transcriptional activation of PXR target genes (di Masi *et al.*, 2009). Thus, failure or decrease in the release of co-repressors upon ligand binding will preclude or diminish transcriptional activation by PXR, even if a ligand is, in principle, able to fully induce a receptor conformation allowing co-activator binding *in vitro*, as it is the case with *para*-hydroxy atorvastatin. This is because the balance of PXR complexes remains with the inactive co-repressor complexes, even after ligand binding (Figure 8).

In this respect, *para*-hydroxy atorvastatin resembles docetaxel, which was shown to recruit co-activators while failing to release co-repressors *in vitro*. However in contrast to the atorvastatin metabolite, docetaxel did not induce PXR target gene expression at all and was thus called a 'PXR-transparent' drug (Synold *et al.*, 2001). *para*-Hydroxy atorvastatin is clearly not such a 'PXR-transparent' compound but it may be regarded as a selective receptor modulator of PXR, as it demonstrates gene and tissue specificity of induction. It induces some PXR target genes (e.g. UGT1A3) as effectively as the parent drug and the other metabolites, while not inducing (e.g. SLCO1B1) or only weakly inducing (e.g. CYP3A4) others.

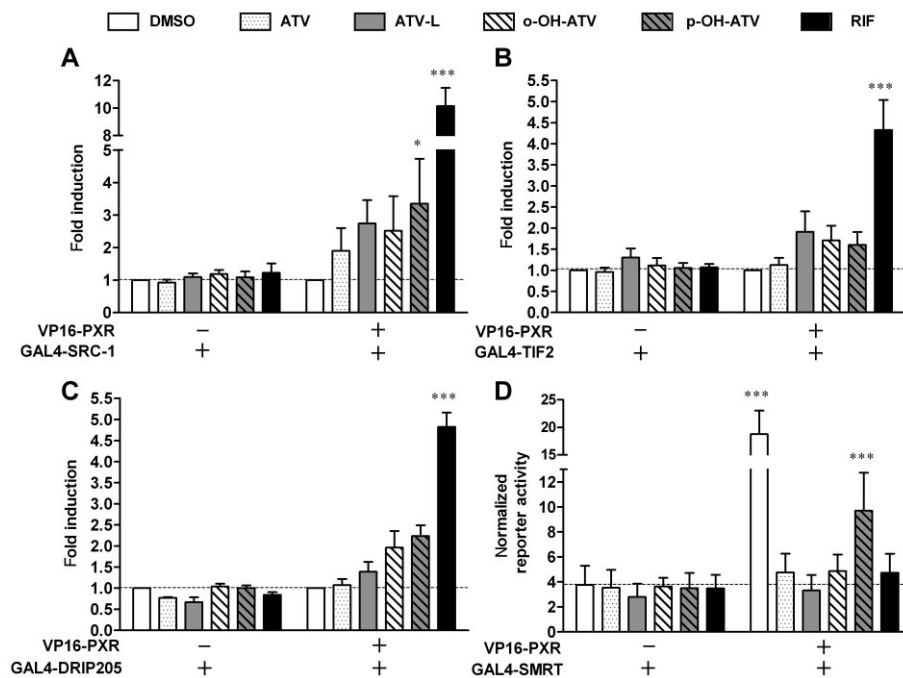


Figure 7

Atorvastatin and its metabolites differentially modulate the interaction of PXR with co-regulators. (A–C) HepG2 cells were co-transfected with expression plasmids encoding GAL4-DBD/co-activator-RID fusion proteins, as indicated, and an expression plasmid encoding VP16-AD/PXR-LBD (108–434) fusion protein (+) or empty expression vector pVP16-AD (-). Columns show the mean fold induction (\pm SD) of the normalized activity of co-transfected pGL3-G5 after 40 h of treatment with 0.1% DMSO, 30 μ M atorvastatin (ATV), 30 μ M atorvastatin lactone, (ATV-L), 30 μ M *ortho*-hydroxy atorvastatin (o-OH-ATV), 30 μ M *para*-hydroxy atorvastatin (p-OH-ATV) and 10 μ M rifampin (RIF). The activity of cells transfected with the respective expression plasmid combination and treated with DMSO only, was designated as 1. (D) HepG2-PXR cells were co-transfected with plasmids encoding GAL4-DBD/SMRT-RID fusion protein and VP16-AD/PXR-LBD (108–434) fusion protein (+) or empty expression vector pVP16-AD (-). Columns show the means (\pm SD) of normalized pGL3-G5 reporter activity after 24 h of treatment with compounds, as described above. Data were analysed by two-way ANOVA with Bonferroni's post-test. *** P < 0.001, * P < 0.05, significantly different from corresponding value with empty expression vector (-).

Furthermore, its inductive capacity also depends on cell type; in contrast to HepG2-PXR cells, *para*-hydroxy atorvastatin proved to be as efficient as the *ortho*-hydroxy metabolite for inducing CYP3A4 promoter activity in the intestinal LS174T cells (data not shown).

Given its impaired activation of PXR in hepatic cell systems, especially regarding the induction of CYP enzymes, *para*-hydroxy atorvastatin might also have a reduced capacity for drug interactions *in vivo*. Induction of CYP3A4 protein expression by *para*-hydroxy atorvastatin is, on average, only 60% of that observed with the *ortho*-hydroxy metabolite. Thus, drug–drug interactions because of CYP3A4 induction may be accordingly diminished if *para*-hydroxy atorvastatin were to be used therapeutically instead of the parent drug. Moreover, the clinical use of an active metabolite, which is no longer subject to metabolism by CYP3A4 itself, would also help to avoid the serious drug interactions, which have been reported for the parent drug atorvastatin, when co-administered with inhibitors or inducers of CYP3A4 (see Neuvonen *et al.*, 2006). The potent selective CYP3A4 enzyme inhibitor itraconazole was reported to increase the area under the plasma concentration time curve (AUC) and elimination half-life of atorvastatin by threefold (Kantola *et al.*, 1998).

Increasing plasma levels of atorvastatin may result in life-threatening muscle toxicity, as reported for the combination of atorvastatin and fluconazole, another inhibitor of CYP3A enzymes (Kahri *et al.*, 2005). On the other hand, the PXR ligand rifampin, a potent inducer of CYP3A expression *in vivo*, decreased the AUC of atorvastatin by 80% (Backman *et al.*, 2005). Additional clinical benefit may result from the potent antioxidant properties of *para*-hydroxy atorvastatin because in contrast to the parent drug, the hydroxy metabolites of atorvastatin protect lipoproteins from oxidation (Aviram *et al.*, 1998).

In conclusion, evidence is provided for the activation of PXR by atorvastatin and its metabolites by demonstrating ligand binding to the receptor. The differential activity of the *para*-hydroxy metabolite in induction of PXR-dependent gene expression, which is most likely caused by impaired co-repressor release, may suggest this active metabolite as a selective PXR modulator and as a promising candidate for future drug development due to its expected lower capacity of drug interactions. This study further demonstrates that it is important to take into account the properties of metabolites when analysing the PXR-dependent induction of drug metabolism and transport.

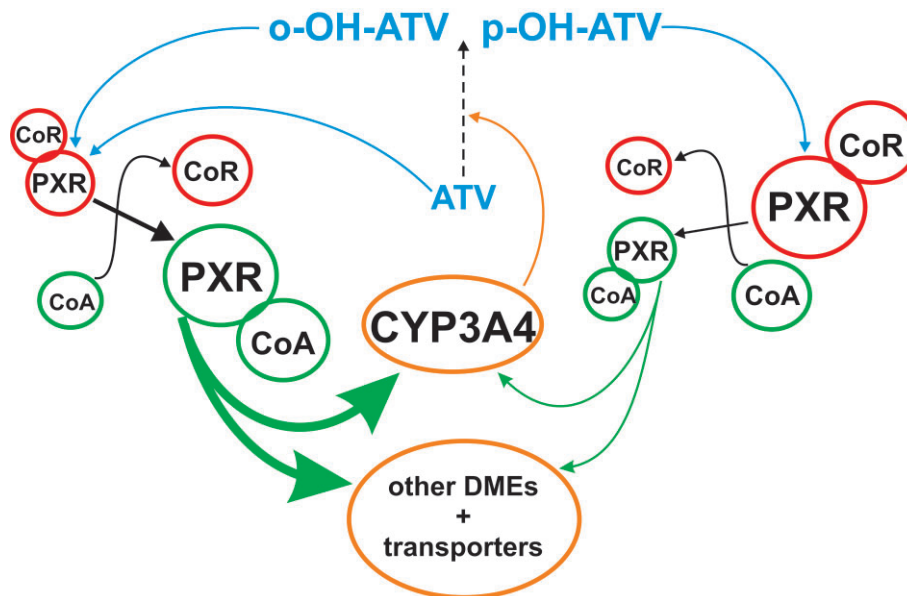


Figure 8

Proposed molecular mechanism of the impaired induction of PXR activation by *para*-hydroxy atorvastatin. Because of the reduced release of co-repressors (CoR), *para*-hydroxy atorvastatin (p-OH-ATV) may result in fewer transcriptionally active PXR-co-activator (CoA) complexes than *ortho*-hydroxy atorvastatin (o-OH-ATV), thereby keeping more PXR in the inactive co-repressor complexes. Consequently, p-OH-ATV results in reduced induction of drug-metabolizing enzymes and transporters.

Acknowledgements

We greatly appreciate the expert technical assistance of K. Abuazi Rincones. We also would like to thank U. Hofmann for drawing the atorvastatin chemical formulas.

This work was supported by the German Federal Ministry of Education and Research (BMBF) HepatosSys network grants 0313081B (A.K.N.), 0313081D (T.S.W and W.E.T.), 0313080F to Rolf Schmid, Institute of Technical Biochemistry, University of Stuttgart, Germany (L.G.) and 0313080I (O.B.), the BMBF grant 03 IS 2061C (M.S.) and the FP7 grant PITN-GA-2009-238132 (M.S.), and by the Robert Bosch Foundation, Stuttgart, Germany.

This work contains parts of the doctoral theses of E.H and L.G.

Conflicts of interest

The authors state no conflicts of interest.

References

- Alexander SPH, Mathie A, Peters JA (2011). Guide to Receptors and Channels (GRAC), 5th edn. Br J Pharmacol 164 (Suppl. 1): S1–S324.
- Arnold KA, Eichelbaum M, Burk O (2004). Alternative splicing affects the function and tissue-specific expression of the human constitutive androstane receptor. Nucl Recept 2: 1.

Aviram M, Rosenblat M, Bisgaier CL, Newton RS (1998). Atorvastatin and gemfibrozil metabolites, but not the parent drugs, are potent antioxidants against lipoprotein oxidation. Arteriosclerosis 138: 271–280.

Backman JT, Luurila H, Neuvonen M, Neuvonen PJ (2005). Rifampin markedly decreases and gemfibrozil increases the plasma concentrations of atorvastatin and its metabolites. Clin Pharmacol Ther 78: 154–167.

Burk O, Tegude H, Koch I, Hustert E, Wolbold R, Glaeser H *et al.* (2002). Molecular mechanisms of polymorphic CYP3A7 expression in adult human liver and intestine. J Biol Chem 277: 24280–24288.

Burk O, Arnold KA, Nussler AK, Schaeffeler E., Efimova E, Avery BA *et al.* (2005). Antimalarial artemisinin drugs induce cytochrome P450 and MDR1 expression by activation of xenosensors pregnane X receptor and constitutive androstane receptor. Mol Pharmacol 67: 1954–1965.

Chen C, Mireles RJ, Campbell SD, Lin J, Mills JB, Xu JJ *et al.* (2005). Differential interaction of 3 hydroxy-3-methylglutaryl-CoA reductase inhibitors with ABCB1, ABCC2, and OATP1B1. Drug Metab Dispos 33: 537–546.

Dring AM, Anderson LE, Qamar S, Stoner MA (2010). Rational quantitative structure-activity relationship (RQSAR) screen for PXR and CAR isoform-specific nuclear receptor ligands. Chem Biol Interact 188: 512–525.

Feidt D, Klein K, Hofmann U, Riedmaier S, Knobeloch D, Thasler WE *et al.* (2010). Profiling induction of cytochrome P450 enzyme activity by statins using a new liquid chromatography-tandem mass spectrometry cocktail assay in human hepatocytes. Drug Metab Dispos 38: 1589–1597.

Geick A, Eichelbaum M, Burk O (2001). Nuclear receptor response elements mediate induction of intestinal MDR1 by rifampin. J Biol Chem 276: 14581–14587.

- Hochman JH, Pudvah N, Qiu J, Yamazaki M, Tang C, Lin JH *et al.* (2004). Interactions of human P-glycoprotein with simvastatin, simvastatin acid, and atorvastatin. *Pharm Res* 21: 1686–1691.
- Horton JD, Goldstein JL, Brown MS (2002). SREBPs: activators of the complete program of cholesterol and fatty acid synthesis in the liver. *J Clin Invest* 109: 1125–1131.
- Howe K, Sanat F, Thumser AE, Coleman T, Plant N (2011). The statin class of HMG-CoA reductase inhibitors demonstrate differential activation of the nuclear receptors PXR, CAR and FXR, as well as their downstream target genes. *Xenobiotica* 41: 519–529.
- Hustert E, Zibat A, Presecan-Siedel E, Eiselt R, Mueller R, Fuss C *et al.* (2001). Natural protein variants of pregnane X receptor with altered transactivation activity toward CYP3A4. *Drug Metab Dispos* 29: 1454–1459.
- Jacobsen W, Kuhn B, Soldner A, Kirchner G, Sewing KF, Kollman PA *et al.* (2000). Lactonization is the critical first step in the disposition of the 3-hydroxy-3-methylglutaryl-CoA reductase inhibitor atorvastatin. *Drug Metab Dispos* 28: 1369–1378.
- Jinno H, Tanaka-Kagawa T, Hanioka N, Ishida S, Saeki M, Soyama A *et al.* (2004). Identification of novel alternative splice variants of human constitutive androstane receptor and characterization of their expression in the liver. *Mol Pharmacol* 65: 496–502.
- Kahri J, Valkonen M, Bäcklund T, Vuoristo M, Kivistö KT (2005). Rhabdomyolysis in a patient receiving atorvastatin and fluconazole. *Eur J Clin Pharmacol* 60: 905–907.
- Kameyama Y, Yamashita K, Kobayashi K, Hosakawa M, Chiba K (2005). Functional characterization of SLCO1B1 (OATP-C) variants, SLCO1B1*5, SLCO1B1*15 and SLCO1B1*15+C1007G, by using transient expression systems of HeLa and HEK293 cells. *Pharmacogenet Genomics* 15: 513–522.
- Kantola T, Kivistö KT, Neuvonen PJ (1998). Effect of itraconazole on the pharmacokinetics of atorvastatin. *Clin Pharmacol Ther* 64: 58–65.
- Keskitalo JE, Kurkinen KJ, Neuvonen PJ, Niemi M (2008). ABCB1 haplotypes differentially affect the pharmacokinetics of the acid and lactone forms of simvastatin and atorvastatin. *Clin Pharmacol Ther* 84: 457–461.
- Kobayashi K, Yamanaka Y, Iwazaki N, Nakajo I, Hosokawa M, Negishi M *et al.* (2005). Identification of HMG-CoA reductase inhibitors as activators for human, mouse and rat constitutive androstane receptor. *Drug Metab Dispos* 33: 924–929.
- Kobayashi K, Saito K, Takagi S, Chiba K (2010). Ligand-dependent assembly of Pregnane X Receptor, constitutive androstane receptor and liver X receptor is applicable to identify ligands. *Drug Metab Lett* 4: 88–94.
- Kocarek TA, Dahn MS, Cai H, Strom SC, Mercer-Haines NA (2002). Regulation of CYP2B6 and CYP3A expression by hydroxymethylglutaryl coenzyme A inhibitors in primary cultured human hepatocytes. *Drug Metab Dispos* 30: 1400–1405.
- Lau YY, Huang Y, Frassetto L, Benet L (2007). Effect of OATP1B transporter inhibition on the pharmacokinetics of atorvastatin in healthy volunteers. *Clin Pharmacol Ther* 81: 194–204.
- Lee YJ, Lee MG, Lim LA, Jang SB, Chung JY (2010). Effects of SLCO1B1 and ABCB1 genotypes on the pharmacokinetics of atorvastatin and 2-hydroxyatorvastatin in healthy Korean subjects. *Int J Clin Pharmacol Ther* 48: 36–45.
- Lennernäs H (2003). Clinical pharmacokinetics of atorvastatin. *Clin Pharmacokinet* 42: 1141–1160.
- Li H, Wang H (2010). Activation of xenobiotic receptors: driving into the nucleus. *Expert Opin Drug Metab Toxicol* 6: 409–426.
- Marino M, di Masi A, Trezza V, Pallottini V, Polticelli F, Ascenzi P (2011). Xenosensors CAR and PXR at work: impact on statin metabolism. *Curr Drug Metab* 12: 300–311.
- di Masi A, De Marinis E, Ascenzi P, Marino M. (2009). Nuclear receptors CAR and PXR: molecular, functional, and biomedical aspects. *Mol Aspects Med* 30: 297–343.
- Monostory K, Pascucci JM, Szabó P, Temesvári M, Köhalmly K, Acimovic J *et al.* (2009). Drug interaction potential of 2-((3,4-dichlorophenethyl)(propyl)amino)-1-(pyridin-3-yl)ethanol (LK-935), the novel nonstatin-type cholesterol-lowering agent. *Drug Metab Dispos* 37: 375–385.
- Neuvonen PJ, Niemi M, Backman JT (2006). Drug interactions with lipid-lowering drugs: mechanisms and clinical relevance. *Clin Pharmacol Ther* 80: 565–581.
- Nussler AK, Nussler NC, Merk V, Brulport M, Schormann W, Yao P *et al.* (2009). The holy grail of hepatocyte culturing and therapeutic use. In: Santin M (ed.). *Strategies in Regenerative Medicine*. Springer: New York, pp. 283–320.
- Omicinski CJ, Coslo DM, Chen T, Laurenzana EM, Peffer RC (2011). Multi-species analyses of direct activators of the constitutive androstane receptor. *Toxicol Sci* 123: 550–562.
- Pasanen MK, Fredrikson H, Neuvonen PJ, Niemi M (2007). Different effects of SLCO1B1 polymorphism on the pharmacokinetics of atorvastatin and rosuvastatin. *Clin Pharmacol Ther* 82: 726–733.
- Pedro-Botet J, Schaefer EJ, Bakker-Arkema RG, Black DM, Stein EM, Corella D *et al.* (2001). Apolipoprotein E genotype affects plasma lipid response to atorvastatin in a gender specific manner. *Atherosclerosis* 158: 183–193.
- Pissios P, Tzamelis I, Kushner P, Moore DD (2000). Dynamic stabilization of nuclear receptor ligand binding domains by hormone or corepressor binding. *Mol Cell* 6: 245–253.
- Poli A (2007). Atorvastatin: pharmacological characteristics and lipid-lowering effects. *Drugs* 67 (Suppl. 1): 3–15.
- Pruksaritanont T, Subramanian R, Fang X, Ma B, Qiu Y, Lin JH *et al.* (2002). Glucuronidation of statins in animals and humans: a novel mechanism of statin lactonization. *Drug Metab Dispos* 30: 505–512.
- Rencurel F, Stenhouse A, Hawley SA, Friedberg T, Hardie DG, Sutherland C *et al.* (2005). AMP-activated protein kinase mediates phenobarbital induction of CYP2B gene expression in hepatocytes and a newly derived human hepatoma cell line. *J Biol Chem* 280: 4367–4373.
- Riedmaier S, Klein K, Hofmann U, Keskitalo JE, Neuvonen PJ, Schwab M *et al.* (2010). UDP-glucuronosyltransferase (UGT) polymorphisms affect atorvastatin lactonization in vitro and in vivo. *Clin Pharmacol Ther* 87: 65–73.
- Sakaeda T, Fujino H, Komoto C, Kakumoto M, Jin JS, Iwaki K *et al.* (2006). Effects of acid and lactone forms of eight HMG-CoA reductase inhibitors on CYP-mediated metabolism and MDR1-mediated transport. *Pharm Res* 23: 506–512.
- Shindo S, Numazawa S, Yoshida T (2007). A physiological role of AMP-activated protein kinase in phenobarbital-mediated constitutive androstane receptor activation and CYP2B induction. *Biochem J* 401: 735–741.
- Sun W, Lee TS, Zhu M, Gu C, Wang Y, Zhu Y *et al.* (2006). Statins activate AMP-activated protein kinase in vitro and in vivo. *Circulation* 114: 2655–2662.

Synold TW, Dussault I, Forman BM (2001). The orphan nuclear receptor SXR coordinately regulates drug metabolism and efflux. *Nat Med* 7: 584–590.

Thasler WE, Weiss TS, Schillhorn K, Stoll PT, Irrgang B, Jauch KW (2003). Charitable state-controlled foundation Human Tissue and Cell Research: ethic and legal aspects in the supply of surgically removed human tissue for research in the academic and commercial sector in Germany. *Cell Tissue Bank* 4: 49–56.

Weiss TS, Pahernik S, Scheruebl I, Jauch KW, Thasler WE (2003). Cellular damage to human hepatocytes through repeated application of 5-aminolevulinic acid. *J Hepatol* 38: 476–482.

Willrich MA, Hirata MH, Hirata RD (2009). Statin regulation of CYP3A4 and CYP3A5 expression. *Pharmacogenomics* 10: 1017–1024.

Wu X, Whitfield LR, Stewart BH (2000). Atorvastatin transport in the Caco-2 cell model: contribution of P-glycoprotein and the proton-monocarboxylic acid co-transporter. *Pharm Res* 17: 209–215.

Yamasaki D, Nakamura T, Okamura N, Kokudai M, Inui N, Takeuchi K *et al.* (2009). Effects of acid and lactone forms of 3-hydroxy-3-methylglutaryl coenzyme A reductase inhibitors on the induction of MDR1 expression and function in LS180 cells. *Eur J Pharm Sci* 37: 126–132.

Supporting information

Additional Supporting Information may be found in the online version of this article:

Figure S1 Expression of PXR and co-factors is maintained in plated primary human hepatocytes. Expression levels of the indicated genes, as determined by TaqMan real-time RT-PCR, were compared between human hepatocytes grown for 5 days as monolayer on collagen I-coated plates and matched freshly isolated cells ($n = 4$). During the last 2 days of culture, hepatocytes were treated with 0.1% DMSO. Data are shown as relative to the expression level in freshly isolated cells, which was designated as 1. Lines indicate means.

Figure S2 CAR ligands induce the assembly of CAR-LBD and *in vitro* interaction with co-activator SRC-1. (A) CAR assembly assay in COS1 cells, which were co-transfected with expression plasmids encoding GAL4-DBD/hCAR-LBD (105–150) and VP16-AD/hCAR-LBD (151–348) fusion proteins. Cells were treated for 40 h with 10 μ M rifampin (RIF), 1 mM phenobarbital (PB), 1 μ M CITCO, 100 μ M clofibrate (CLO), 30 μ M triphenylphosphate (TPP), 10 μ M clotrimazole (CLOT), 10 μ M PK11195 (PK) or 0.1% DMSO only. Mean fold induction (\pm SD) of the normalized activity of co-transfected reporter plasmid pGL3-G5 by treatment with the indicated

chemicals is shown. Hatched and cross-hatched columns indicate treatment with negative controls. Columns in black or grey indicate treatment with agonists or inverse agonists respectively. The respective activity of cells treated with DMSO only, was designated as 1. (B) Biacore analysis of ligand-induced interaction of co-activator SRC-1 with CAR *in vitro*. CAR-LBD protein, pre-incubated with 100 μ M of the indicated chemicals or 1% DMSO only, was injected onto immobilized SRC-1-RID protein (open columns). As a control, chemicals were also injected alone (filled columns). Data are shown as means \pm SD of three to six independent experiments. Open columns show increase in binding by pre-incubation of CAR with chemicals. Binding of CAR to SRC-1 in the presence of DMSO only, was designated as 1. (A) and (B) Statistically significant differences were analysed by one sample *t*-test, resulting *P*-values were corrected for multiple testing by the method of Bonferroni and indicated by asterisks (* $P < 0.05$; ** $P < 0.01$; *** $P < 0.001$).

Figure S3 Atorvastatin and its metabolites do not change the interaction of CAR with co-regulators. (A–C) COS1 cells were co-transfected with expression plasmids encoding GAL4-DBD/co-activator-RID fusion proteins, as indicated, and expression plasmids encoding VP16-AD/CAR-LBD (105–348) (A) and (B) or VP16-AD/CAR-SV2-LBD (105–353) (C) fusion proteins (open columns) or empty expression vector pVP16-AD (filled columns). Cells were treated for 40 h with 1 μ M CITCO, 30 μ M of atorvastatin metabolites or 0.1% DMSO only. Mean fold activation (\pm SD) of the normalized activity of co-transfected reporter plasmid pGL3-G5 by treatment with the indicated chemicals is shown. The respective activity of cells transfected with the particular GAL4-DBD/co-activator-RID fusion protein expression plasmids and pVP16-AD, treated with DMSO only, was designated as 1. (D) COS1 cells were co-transfected with plasmids encoding GAL4-DBD/SMRT-RID fusion protein and VP16-AD/CAR-LBD (105–348) fusion protein. An expression plasmid encoding human RXR α was additionally co-transfected. Columns show the mean fold activation (\pm SD) of normalized pGL3-G5 reporter activity after 40 h of treatment with chemicals (AND, 10 μ M androstrenol), as compared with the respective activity of cells transfected with GAL4-DBD/SMRT-RID plasmid and pVP16-AD, treated with DMSO only, which was designated as 1. (A–D) Statistical significant differences to DMSO vehicle treatments were analysed by repeated measures one-way ANOVA with Dunnett's multiple comparisons test and indicated by asterisks (** $P < 0.01$).

Table S1 Hepatocyte donor data

Table S2 Oligonucleotides for quantitative real-time RT-PCR

Please note: Wiley-Blackwell are not responsible for the content or functionality of any supporting materials supplied by the authors. Any queries (other than missing material) should be directed to the corresponding author for the article.